Available online at www.sciencedirect.com
SCIENCE DIRECT®
Polymer 44 (2003) 5803–5809
polymer
www.elsevier.com/locate/polymer

Investigating polymer crystallization by time-dependent light scattering: a direct approach in the data analysis applied for s-polypropylene

A. Hoffmann, G. Strobl*

Fakultat für Physik, Physikalisches Institut, Albert-Ludwigs-Universität, 79104 Freiburg, Germany

Received 6 May 2003; received in revised form 10 June 2003; accepted 18 June 2003

Abstract

We developed a procedure for a direct evaluation of light scattering patterns registered during an isothermal crystallization of s-polypropylene. Analysis is based on the determination of three parameters of the scattering curve for both, polarized and depolarized measuring conditions: (i) the forward scattering intensity $I(q \rightarrow 0)$ (ii) the width Δq of the intensity distribution (iii) the integral intensity in the registration plane, Q_2. We derive equations for these parameters and relate them to the size and the inner structure of the hedrites which develop in s-polypropylene during a crystallization.

Keywords: Polymer crystallization; Light scattering patterns; Scattering intensity

1. Introduction

Light scattering is a particularly sensitive tool for detecting small density variations in initially homogeneous systems and can therefore be used in time dependent studies of polymer crystallization to encompass a large development range, from the initial stages to the final state where the sample volume is covered by the fully grown objects. In recent time there have been several attempts to observe with light scattering in particular the early stages of crystallization, in studies of Okada et al. [1], Pogodina et al. [2], and in several works by Imai, Matsuba, Kaji et al. [3,4].

Different from the case of small angle X-ray scattering, data evaluation in light scattering experiments cannot be carried out employing standard procedures. In SAXS experiments one always encounters crystalline lamellae with nanometer-thickness as basic structural units and then consequently uses the (1D-) correlation function approach, in light scattering experiments the situation is different. The larger, micrometer-sized objects vary in their form and their inner structure, between different systems and also with time. Spherulites and hedrites are only two limiting cases, and there exist more morphological forms and various intermediate states. Corresponding to this situation also data treatments vary. An article by Haudin in Ref. [6] provides an excellent overview. If the structure factor of the object is known, as in the case of spherulites, data evaluation can be carried out by a data fitting. It yields the object size and parameter proportional to local birefringence and density. As an alternative, there exist direct 'statistical' approaches which employ correlation functions. Strictly speaking, these can only be applied for objects with isotropic scattering, because they are based on an isotropic correlation function, but this is rarely the case. The method is, however, still applied. The results—one obtains the mean-squared fluctuations of the density and the local anisotropy—are approximate, but useful.

We describe in this paper a data analysis procedure with some new features which we developed in the course of light scattering experiments on crystallizing syndiotactic polypropylene (sPP). It is generally applicable for growing hedrites which are found in this case. After some theoretical explanations we exemplify the use for one isothermal crystallization. The results of the complete study—an investigation of the structural changes in sPP during the crystallization process, conducted at various temperatures—are presented separately.

2. Instrumentation and sample

With the aid of a homebuilt apparatus a simultaneous registration of polarized and depolarized light scattering patterns during an isothermal crystallization process was achieved. Its basic set-up is shown in Fig. 1. Scattering is

* Corresponding author.
E-mail address: strobl@uni-freiburg.de (G. Strobl).

0032-3861/03/$ - see front matter © 2003 Elsevier Ltd. All rights reserved.
doi:10.1016/S0032-3861(03)00572-X

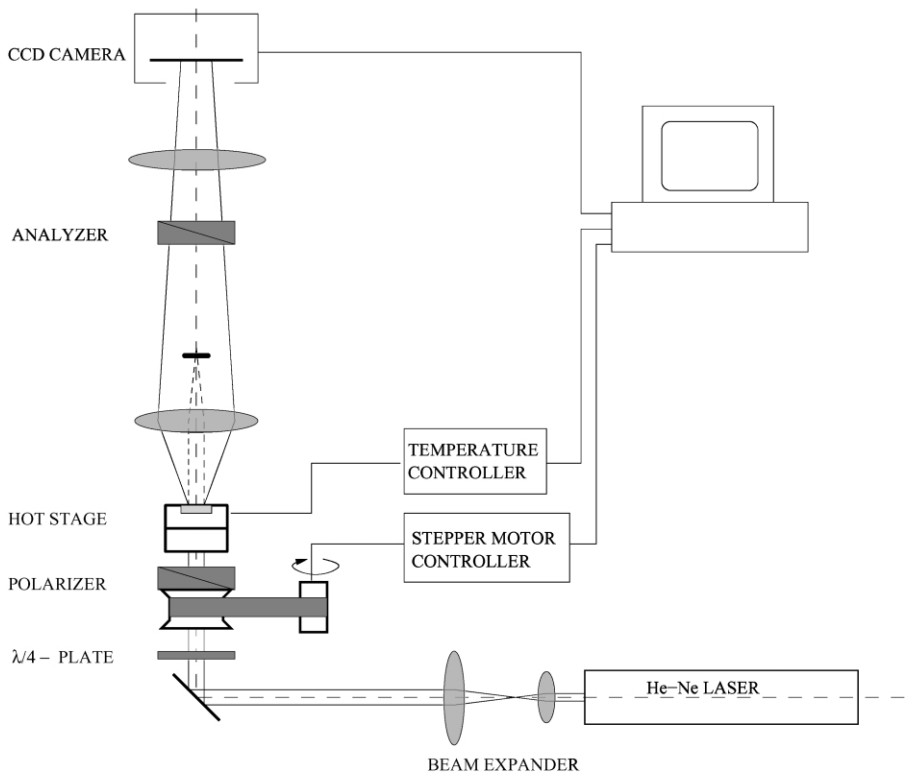

Fig. 1. Set-up of the light scattering apparatus used for a simultaneous registration of vv and hv-scattering curves.

induced by a He–Ne-laser; the beam cross-section is expanded to cover a larger sample area. By employing a polarizer placed after a λ/4-plate which can be rotated by a stepping motor, the polarization direction of the incident light is selected. Keeping the analyzer direction fixed one can rapidly switch from parallel (vv) to perpendicular (hv) conditions and thus quasi-simultaneously register polarized and depolarized light scattering patterns. The patterns are registered by a CCD-camera. Samples are kept at a fixed temperature in a hot stage. A PC collects all data and controls both the temperature and the direction of the polarizer.

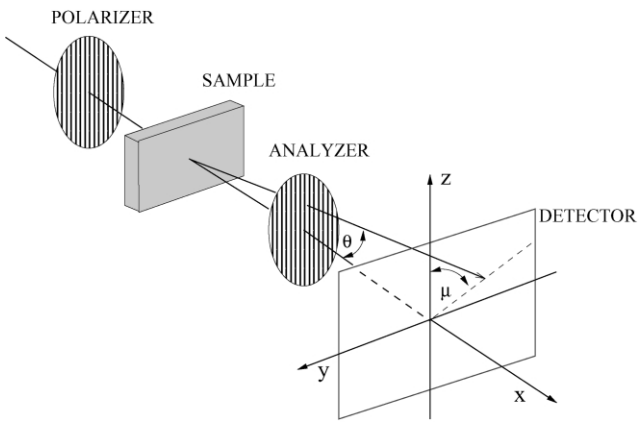

Fig. 2. Scattering geometry: the incident laser beam propagates along x. Scattered light is registered in the q_y, q_z-plane for polarizer directions along z (vv-) and y (hv-scattering); the analyzer direction is fixed along z.

Fig. 2 shows the scattering geometry and defines the coordinate system. The laser beam propagates in x-direction. The scattering pattern taken up by the camera represents the scattering intensity $I(0, q_y, q_z)$ in the q_y, q_z-plane.

The sample of sPP used in the studies was a commercial brand supplied by FINA Oil, Brussels. It has 83% syndiotactic pentades and a molar mass $M_w = 6 \times 10^4$ g × mol^{-1} ($M_w/M_n = 4$). We had used this material previously in investigations of the deformation behavior which also included a structural characterization [5].

3. Scattering patterns of hedrites: general appearance

Fig. 3 shows on the left-hand side a series of polarized (vv) scattering patterns and on the right-hand side depolarized (hv) scattering patterns. They were obtained at different times during an isothermal crystallization at 104 °C subsequent to a rapid cooling of a melt first kept at 150 °C. As can be noted, the hv-scattering shows a maximum in forward direction, which is, however, covered by a beam stop. This property indicates that the objects which scatter the light possess an essentially uniform chain orientation, i.e. resemble hedrites rather than spherulites; spherulites would produce a maximum at some finite angle and, ideally, a vanishing scattering intensity at $q = 0$. That sPP forms hedrites is well-known from microscopic observations and here confirmed again.

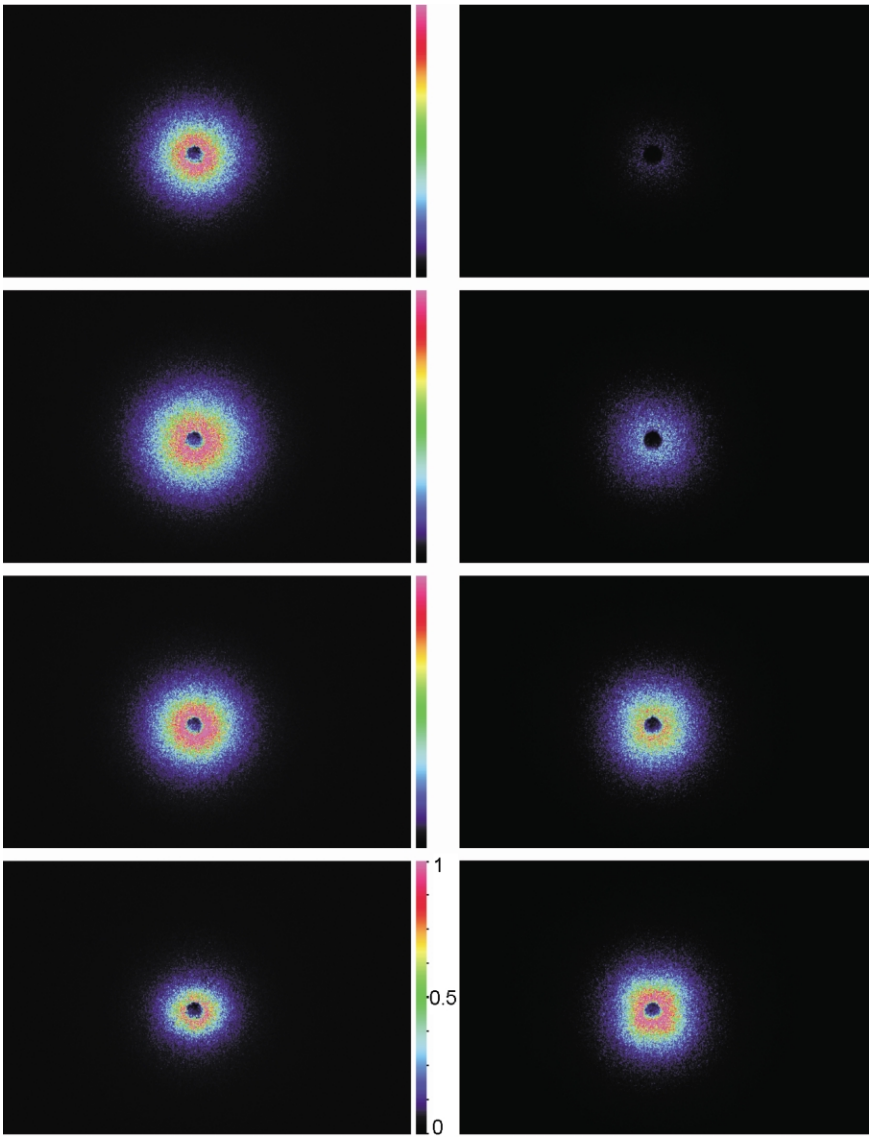

Fig. 3. sPP: vv-(left) and hv-(right) light scattering patterns registered crystallization at $T_c = 104$ °C ($T_m = 150$ °C). The patterns were obtained after 1800 s (top), 2400, 3000, and 3600 s (bottom).

The hv-scattering patterns appear isotropic at the initial stages and develop later a slight anisotropy. This anisotropy indicates that the individual objects produce—due to their anisometric shape—a non-isotropic scattering intensity distribution. In spite of the random orientational distribution of the objects in space no isotropic hv-scattering results. The intensity distribution of the light scattered by a single object i is given by

$$I_i^{hv}(\mathbf{q}) \sim |\int_{\text{obj } i} \delta\alpha_{yz}(\mathbf{r})\exp(i\mathbf{qr})d^3\mathbf{r}|^2 \quad (1)$$

where $\delta\alpha_{yz}$ denotes the difference between the (constant) yz-component of the polarizability tensor within the object, and the polarizability of the isotropic melt. $\delta\alpha_{yz}$ and, correspondingly, I_i^{hv} depend on the orientation of the object relative to the space fixed coordinate-system. Orientations where the chain axis is inclined by 45° against the z-axis lead to the highest $\delta\alpha_{yz}$ and the associated intensity distribution $I_i^{hv}(\mathbf{q})$ thus stands out in the scattering diagram. The final hv-scattering pattern shows this property.

In a weaker form the same effect is also found in $I^{vv}(\mathbf{q})$. This intensity distribution is here given by

$$I_i^{vv}(\mathbf{q}) \sim |\int_{\text{obj } i} \delta\alpha_{zz}(\mathbf{r})\exp(i\mathbf{qr})d^3\mathbf{r}|^2 \quad (2)$$

As explained later in more detail, $\delta\alpha_{zz}$ includes in addition to the orientational independent component related to the density difference between the objects and the surrounding melt also a second component which is associated with the birefringence of the chains. In this case object orientations with the chain axis parallel or perpendicular to z produce the highest intensity. Hence, one expects a deviation from an isotropic scattering pattern with some elongation along q_z and q_y.

The general features of the scattering patterns suggest to base the data analysis on six parameters, namely, separately for vv and hv-scattering

- the integral scattering intensity in the q_y, q_z-plane

$$Q_2 = \int I(0, q_y, q_z) \mathrm{d}q_y \mathrm{d}q_z \tag{3}$$

- the scattering in forward direction $I(q \rightarrow 0) = I_0$,
- the correlation length l of the evolving structure which is reciprocal to the half width of the (2D-) scattering intensity distribution $I(0, q_y, q_z)$.

3.1. Employing the Debye–Bueche structure factor

We found that throughout the whole crystallization process the scattering patterns produced by sPP were always rather well represented by the Debye–Bueche structure factor

$$I(q) = \frac{I_0}{(1 + l^2 q^2)^2} \tag{4}$$

where l is a correlation length characterizing the object's size. A typical example is given in Fig. 4. The data were obtained during the crystallization at 104 °C from a melt which was at first kept for 20 min at $T_m = 150$ °C. Measured intensities were averaged over all points with the same

$$q = (q_y^2 + q_z^2)^{1/2} \tag{5}$$

and then plotted in the form $I^{-1/2}$ versus q^2 as suggested by the Debye–Bueche function. One obtains for the depolarized scattering for all times straight lines in accord with Eq. (4), and for the polarized scattering lines with some curvature. As shown by this representation, the maximum in the scattering intensity occurs always for $q = 0$. An extrapolation of the intensity to the origin in order to determine I_0 is always possible, even when curves show some curvature. Using the Debye–Bueche related representation also for extrapolations to $q \rightarrow \infty$ one can determine also the (2D-) integral scattering intensity Q_2 (Eq. (3)). Q_2 and I_0 yield together the correlation length l. We use the equation

$$Q_2 = \pi \frac{I_0}{l^2} \tag{6}$$

valid for the Debye–Bueche structure factor.

4. Theory: I_0, Q_2 and l in the Rayleigh–Gans approximation

What is the accurate meaning of I_0, Q_2 and l in the two cases, hv and vv-scattering, what can be deduced from them? To give the answer we employ, as usual in light scattering experiments of polymers the Rayleigh–Gans approximation (compare, for example, the article of Haudin in Ref. [6]). We begin with a splitting of the ij-component of the polarizability—precisely, its difference to the melt polarizability—in an isotropic and an anisotropic part, as

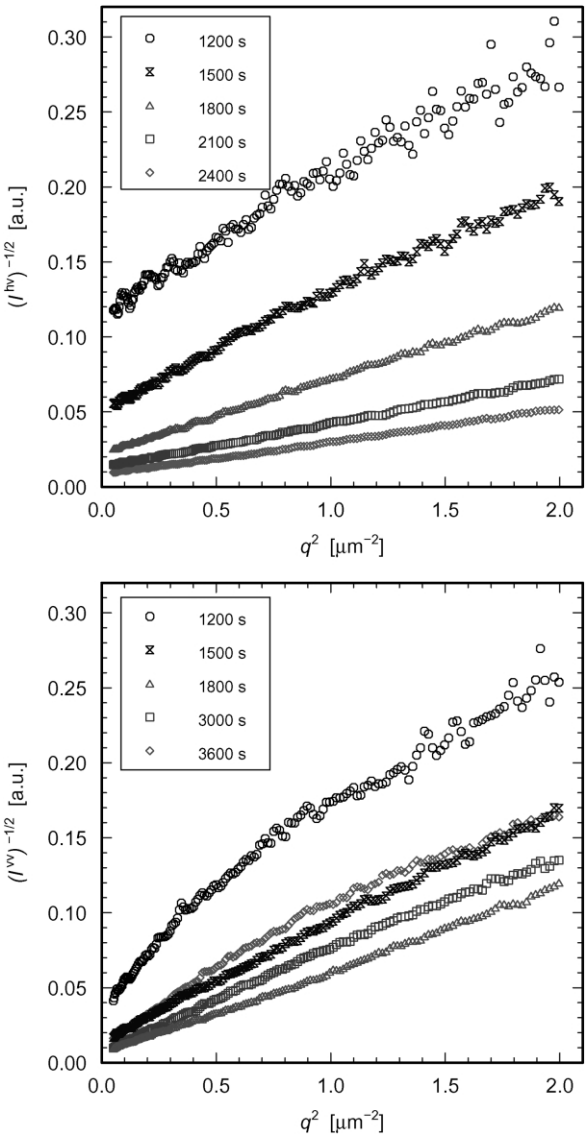

Fig. 4. sPP, crystallizing at 104 °C after cooling a melt kept at 150 °C. Intensities $I(q)$ of vv and hv-scattering at the indicated times of structure evolution, represented according to the Debye–Bueche function.

$$\delta\alpha_{ij} = \delta\alpha_{ij}^{\mathrm{is}} + \delta\alpha_{ij}^{\mathrm{an}} \tag{7}$$

The isotropic part produces only contributions on the tensor diagonal

$$\delta\alpha_{ij}^{\mathrm{is}} = \delta_{ij} \cdot \delta\alpha^{\mathrm{is}} \tag{8}$$

For each ij-component of the anisotropic part the average over all orientations vanishes

$$\overline{\delta\alpha_{ij}^{\mathrm{an}}} = 0 \tag{9}$$

A general equation relates in all scattering experiments—light, X-ray or neutron-scattering—the mean-squared

fluctuation of the scattering length, here represented by the polarizability per unit volume, with the integral of the scattering intensity over the reciprocal space. Application of this general relation to the case of hv-light-scattering yields for our experiment the equation

$$\langle(\delta\alpha_{yz}^{an})^2\rangle \sim \int I^{hv}(q_x, q_y, q_z)\mathrm{d}q_x\mathrm{d}q_y\mathrm{d}q_z = Q_3^{hv} \tag{10}$$

where the brackets $\langle\ \rangle$ denote the volume average. As we do not determine the scattering intensities outside the $q_x = 0$-plane we have only a knowledge of the two-dimensional integral Q_2 defined by Eq. (3). This two-dimensional and the three-dimensional integral Q_3^{hv} are related by

$$Q_3^{hv} \simeq Q_2^{hv}\Delta q \tag{11}$$

where Δq describes the (integral)width of the scattering curve along q_x. For the observed, nearly isotropic scattering we can write

$$\Delta q \simeq \frac{1}{l^{hv}} \tag{12}$$

Since we have to distinguish between the correlation lengths measured in hv and vv-scattering experiments, we add to l a corresponding superscript. Hence, the meaning of the quantity Q_2^{hv} taken from the experiments is described by

$$Q_2^{hv} \sim \langle(\delta\alpha_{yz}^{an})^2\rangle l^{hv} \tag{13}$$

If no correlation exists between the orientations of different objects, and if these objects occupy a fraction ϕ of the volume, we can represent the volume average of Eq. (13) as

$$\langle(\delta\alpha_{yz}^{an})^2\rangle = \phi\overline{(\delta\alpha_{ij}^{an})^2} \tag{14}$$

As previously, the overline on the right-hand side of the equation expresses an average over all orientations which an object can have. For n objects per unit volume the volume fraction ϕ occupied by them can be written as

$$\phi \simeq n(l^{hv})^3 \tag{15}$$

which leads to

$$Q_2^{hv} \sim n(l^{hv})^4\overline{(\delta\alpha_{yz}^{an})^2} \tag{16}$$

and for the end value to

$$Q_2^{hv}(t \to \infty) \sim l^{hv}(\infty)\overline{(\delta\alpha_{yz}^{an})^2} \tag{17}$$

An expression for the forward scattering I_0^{hv} can be directly given. For a random orientational distribution of the objects without any next neighbor correlations the total intensity is the sum of the intensities of all objects,

$$I_0^{hv} \sim \overline{n\left(\int_{obj}\delta\alpha_{yz}^{an}\,\mathrm{d}^3\mathbf{r}\right)^2} \tag{18}$$

$$I_0^{hv} \simeq n(l^{hv})^6\overline{(\delta\alpha_{yz}^{an})^2} \tag{19}$$

What is the meaning of l^{hv}? The answer simply is: it represents a measure for the object size.

Next, we consider the parameters Q_2^{vv}, I_0^{vv} and l^{vv}, as they follow from the vv-scattering curves. The integral of the intensity of polarized scattering over the reciprocal space is determined by the mean-squared fluctuation of the zz-component of the polarizability, $\delta\alpha_{zz}$, as

$$\langle\delta\alpha_{zz}^2\rangle - \langle\delta\alpha_{zz}\rangle^2 \sim Q_3^{vv} = \int I^{vv}(q_x, q_y, q_z)\mathrm{d}q_x\mathrm{d}q_y\mathrm{d}q_z \tag{20}$$

We again relate the experimentally determined quantity Q_2^{vv} to Q_3^{vv} by writing

$$Q_2^{vv} \simeq Q_3^{vv}l^{vv} \tag{21}$$

analogous to Eqs. (11) and (12) in the case of the hv-scattering. For internally homogeneous objects we can write for the mean-squared fluctuation in the absence of any orientational correlations

$$\langle\delta\alpha_{zz}^2\rangle - \langle\delta\alpha_{zz}\rangle^2 = \phi(1-\phi)(\delta\alpha^{is})^2 + \phi\overline{(\delta\alpha_{zz}^{an})^2} \tag{22}$$

The first term on the right-hand side describes, as is well known, the density fluctuations in two-phase structure (compare, for example, Ref. [7], p. 410). These pass over a maximum for equal, i.e. 50%, fractions of the two phases. Since the observed hedrites are internally anisotropic, the second contribution proportional to the volume fraction of the hedrites arises, having the same form as Eq. (14) for the hv-scattering. In the limiting case of a small volume fraction of the hedrites Eq. (22) turns into

$$Q_2^{vv} \sim n(l^{vv})^4[(\delta\alpha^{is})^2 + \overline{(\delta\alpha_{zz}^{an})^2}] \tag{23}$$

when using for ϕ an expression analogous to Eq. (15). As one usually finds

$$\delta\alpha^{is} \gg |\delta\alpha_{zz}^{an}| \tag{24}$$

it is in good approximation

$$Q_2^{vv} \sim n(l^{vv})^4(\delta\alpha^{is})^2 \tag{25}$$

In the other limit, for long times, when the sample is completely covered with hedrites, one ends up at the expression

$$Q_2^{vv} \sim l^{vv}(\infty)\overline{(\delta\alpha_{zz}^{an})^2} \tag{26}$$

which relates to the anisotropic part in the zz-scattering only. The expression includes as one parameter the final correlation length $l^{vv}(\infty)$ which represents a measure for the final size of the hedrites.

For I_0^{vv} one can write down expressions for the initial and final stage,

$$I_0^{vv} \sim n(l^{vv})^6(\delta\alpha^{is})^2 \tag{27}$$

and

$$I_0^{vv}(t \to \infty) \sim n(l^{vv}(\infty))^6\overline{(\delta\alpha_{zz}^{an})^2} \tag{28}$$

in correspondence to Eq. (19).

5. Results and discussion

Fig. 5 shows the six parameters derived from the scattering data, I_0, Q_2 and l both for hv and the vv-scattering, as they vary with time during the crystallization process.

The observations for the hv-scattering are conceivable on the basis of the derived equations. One expects a steady increase in Q_2^{hv}, I_0^{hv} and l^{hv} to their final values, which is observed. One minor modification arises, as the time dependence of the correlation length includes some fluctuation. This indicates that the orientations are not ideally random. Apparently a short range order between neighbors exists, which is not surprising for the planar hedrites. Apart from this effect one observes a steady increase in the correlation length with time at the begin and a convergence to a final value

$$l^{hv}(t \to \infty) = 2.8 \text{ nm}$$

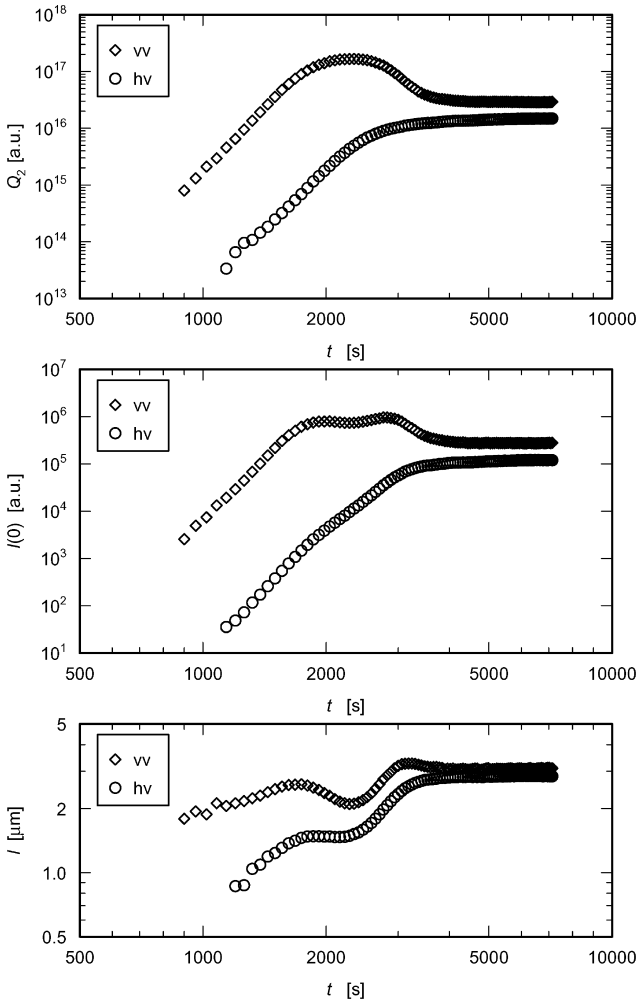

Fig. 5. sPP, crystallizing at 104 °C after cooling a melt kept at 150 °C. Results derived from Fig. 4 and analogous curves at intermediate times. Variations with time of the integral scattering intensities in the (q_y, q_z)-plane, Q_2^{vv} and Q_2^{hv} (top), the intensities of forward scattering I_0^{vv} and I_0^{hv} (center) and the correlation lengths l^{vv} and l^{hv} (bottom).

The change with time of Q_2^{vv} as shown in the top part of Fig. 5 is also conceivable. Q_2^{vv} first increases, then passes over a maximum and ends at a certain final value. This arises because a scattering caused by density variations cannot discriminate between objects and holes. At the begin the scattering is due to the objects, but later it turns over to a scattering of the holes, which is also isotropic. At the end, when the hedrites fill the sample completely, there remains only the birefringence contribution, as given by Eq. (26). As expected, this final value is comparable to the final value of Q_2^{hv} given by Eq. (17).

How can we understand the time dependence of l^{vv}? It begins with a linear increase, then goes over two maxima and ends at a non-vanishing final value. Here different effects are superposed. First, consider the case of a pure density fluctuation scattering, i.e.

$$\delta\alpha_{zz}^{an} = 0 \tag{29}$$

For such a system with two isotropic phases the correlation length has to include length scales of both phases. Theory leads to the expression (compare, for example, Ref. [8])

$$\frac{1}{l^{vv}} = \frac{1}{l_a} + \frac{1}{l_{obj}} \tag{30}$$

where l_a and l_{obj} describe the mean lengths of a segment along a ray intercepted by the melt or by hedrites, respectively. For

$$l_{obj}/l_a \ll 1 \tag{31}$$

we may write for the correlation length

$$l = l_{obj}\frac{1}{1 + (l_{obj}/l_a)} \approx l_{obj} \tag{32}$$

According to this equation the correlation length represents the size of the hedrites only, if they are sufficiently small. In the further course of the evolution the value of the correlation length is reduced compared to the size of the hedrites, and then passes over a maximum. Considering the situation in the other limit—the presence of small holes between the nearly fully grown hedrites—we write

$$l^{vv} = l_a\frac{1}{1 + (l_a/l_{obj})} \tag{33}$$

Now the correlation length represents the hole size and again becomes reduced against this value if the holes become larger. Between the two maxima in l^{vv} one finds for

$$l^{vv} \approx l_{obj} \approx l_a \tag{34}$$

a minimum. The measured curve $l^{vv}(t)$ represents a superposition of the thus described density scattering with an anisotropy scattering. The latter contribution leads to a curve similar to $l^{hv}(t)$. Therefore, we find also for the vv-scattering a non-vanishing final value of l^{vv}, which is similar to l^{hv}.

Why do we observe at the beginning a clear difference

between l^{vv} and l^{hv} of about a factor 2, although they relate both to the same objects, the hedrites? The effect is due to the already mentioned orientational dependence of the light scattering of these anisotropic particles. For hv-scattering a maximum arises when the surface normal of the hedrites is in the *yz*-plane, enclosing an angle of 45° with the *z*-axis. No depolarized scattering at all arises if the orientation of the normal is along the *x*-axis. As a consequence, the value measured for l^{hv} includes two different length scales, the thickness of the hedrites in chain direction and the much larger lateral extension. For the vv-scattering one has another situation. Here, those hedrites which have their surface normal oriented along the *x*-direction *do* contribute to the scattering. As a consequence, the correlation length l^{vv} will become larger than the correlation length l^{hv} in case of the depolarized scattering.

Hence, all the basic features showing up in the curves in Fig. 5 are conceivable. Scattering arises from internally homogeneous anisotropic objects, the hedrites, which grow in time, finally filling the whole sample. The kinetics can be described by one characteristic time τ, which can be chosen as the one required to achieve a 50% coverage of the sample by the hedrites. In the given example this time amounts to $\tau = 2300$ s. There is, however, also a peculiar observation. For the usual case of a constant number of growing nuclei, i.e. $n =$ constant, one expects according to Eq. (16) for a linear increase in the object diameter an increase of Q_2 and I_0 according to the power laws

$$Q_2^{vv} \sim Q_2^{hv} \sim t^4, \qquad I_0^{vv} \sim I_0^{hv} \sim t^6 \tag{35}$$

The observation greatly differs from this expectation. We find

$$Q_2^{vv} \sim Q_2^{hv} \sim t^{7.5}, \qquad I_0^{vv} \sim I_0^{hv} \sim t^{9.5} \tag{36}$$

The observed larger exponent indicates that the inner composition of the hedrite as given by the packing density of the constituent lamellae, is not constant but increases steadily in the time range of the experiment. Indeed, this is quite reasonable as it has often been observed, in particular in recent time with the aid of atomic force microscopes. A filling-in of subsidiary lamellae, subsequent to the formation of a primary, more open structure set-up by dominant lamellae, is often observed. The experiments just cover a factor of 2 in time, which implies an increase by a factor $2^{(4.5-3)} \approx 3$ in the packing density.

Acknowledgements

Support of this work by the Deutsche Forschungsgemeinschaft is gratefully acknowledged. Thanks are also due to the 'Fonds der Chemischen Industrie' for financial help.

References

[1] Okada T, Saito H, Inoue T. Macromolecules 1992;25:1908.
[2] Pogodina NV, Siddiquee SK, van Egmond JW, Winter HH. Macromolecules 1999;32:1167.
[3] Matsuba G, Kaji K, Nishida K, Kanays T, Imai M. Polym J 1999;31:722.
[4] Imai M, Kaji K, Kanaya T, Sakai Y. Phys Rev B 1995;52:12696.
[5] Men Y, Strobl G. J Macromol Sci—Phys 2001;B40:775.
[6] Haudin JM. In: Meeten GH, editor. Optical properties of polymers. Amsterdam: Elsevier; 1986.
[7] Strobl G. The physics of polymers. Berlin: Springer; 1997. p. 410.
[8] Alexander LE. X-ray diffraction methods in polymer science. New York: Wiley; 1997. p. 297.